



Organo-Metallic Palladium Complexes used for CO₂ Storage and Environmental Remediation

Zinah N. Mahmood¹ | Mahasin Alias¹ | Emad Yousif^{2✉} | Shaymaa R. Baqer¹ | Mohammed Kadhom³ | Dina S. Ahmed⁴ | Ahmed Ahmed⁵ | Amani A. Husain⁵ | Rahimi M. Yusop⁶ | Ali H. Jawad⁷

1. Department of Chemistry, College of Science for Women, University of Baghdad, Baghdad, Iraq

2. Department of Chemistry, College of Science, Al-Nahrain University, Baghdad, Iraq

3. Department of Environmental Science, College of Energy and Environmental Science, Al-Karkh University of Science, Baghdad, Iraq

4. Department of Medical Instrumentation Engineering, Al-Mansour University College, Baghdad, Iraq

5. Polymer Research Unit, College of Science, Al-Mustansiriyah University, Baghdad, Iraq

6. School of Chemical Sciences and Food Technology, Faculty of Science and Technology, Universiti Kebangsaan Malaysia, Bangi, Selangor, Malaysia

7. Faculty of Applied Sciences, Universiti Teknologi MARA, 40450, Shah Alam, Selangor, Malaysia

Article Info

Article type:

Research Article

Article history:

Received: 18 Sep 2022

Revised: 19 Nov 2022

Accepted: 19 Jan 2023

Keywords:

Sodium fusidate

Transition metal

Gas separation

Gas storage

Gases uptake

ABSTRACT

Gas storage is an important branch of technology that has many economic and environmental aspects. This technique could save gas to the need time and contribute to solving the CO₂ and global warming problems. In this work, the structure and physico-chemical properties of the prepared palladium complex were characterized in the solid and solution states using spectroscopic techniques. These examination methods include ultraviolet-visible (UV-Vis), Fourier transform infrared (FTIR), metal and elemental analyses, and measurements of magnetic susceptibility and conductivity at room temperature. Also, findings on the surface morphology and surface area were provided via Field emission scanning electron microscopy (FESEM) and Brunauer–Emmett–Teller (BET) techniques, respectively. High-pressure adsorption measurements were investigated by storing carbon dioxide, and the results proved that such materials own remarkable gas adsorption properties that make them a good option for gas separation and storage. Gases uptake at 323 K for the complexes leads to the highest CO₂ uptake. The prepared material could pave the road for further exploitation of similar materials.

Cite this article: Mahmood, Z.N., Alias, M., Yousif, E., Baqer, Sh.R., Kadhom, M., Ahmed, D.S., Ahmed, A., Husain, A.A., Yusop R.M., & Jawad A.H. (2023). Organo-Metallic Palladium Complexes used for CO₂ Storage and Environmental Remediation. *Pollution*, 9 (2), 693-701.

<http://doi.org/10.22059/POLL.2022.348855.1632>



© The Author(s).

Publisher: University of Tehran Press.

DOI: <http://doi.org/10.22059/POLL.2022.348855.1632>

INTRODUCTION

Sodium fusidate, commonly called Fusidic acid (FA), is a hydrophobic antibiotic used to treat bacterial infections of sensitive osteomyelitis, skin, and soft tissues [Fernandes, 2016]. Fusidic acid is crucial in clinics due to its reliability in combining with a wide range of antibiotics [Whitby, 1999]. This could be explained as the drug shows fine toxicity and bacterial resistance [Curbete and Salgado, 2015]. Yet, FA is assumed as the most important component among

*Corresponding Author Email: emad_yousif@hotmail.com

the fusidane group. This group is considered a small class of tetracyclic nor-triterpenes that possesses a cyclopentanoperhydrophenanthrene ring and belongs to the steroid compounds [Curbete and Salgado, 2015].

The increasing global need for energy is associated with the growing number of populations, where fossil fuel (oil, gas, and coal) is considered the dominant energy source until now. However, this fuel negatively contributes to air quality and health; global warming is one of the resulting problems that links several recent natural disasters worldwide [Mahmood et al., 2021; Owusu and Asumadu-Sarkodie, 2016; Al-Furaiji et al., 2020]. Over time, oil and natural gas consumption shows an increase due to the increasing energy demand, and carbon emissions are raising to unrivaled levels. High CO₂ concentration in the air is attributed to multiple serious problems [Lim et al., 2010], global warming is the main one, followed by pollution, climate change, and natural disasters [Owusu and Asumadu-Sarkodie, 2016; Al-Furaiji et al., 2018; Waisi et al., 2015].

The utilization of solids for gas storage is a recent technology that gains attention because of its wide applications [Morris and Wheatley, 2008]. This technology presents a reliable solution to handle the fluctuation in demand and supply. With this technology, gas could be injected into a storage material at low demand periods and released when the demand increases [Safarov and Atkinson, 2017]. Furthermore, high CO₂ concentrations might be mitigated via carbon capturing and storage (CCS) techniques [Benson and Orr, 2008]. Compared with alternative methods, this technique is a cost-effective option that efficiently reduces CO₂ emissions and, ultimately, climate change [Xenias and Whitmarsh, 2018].

In this paper, sodium fusidate was used as a ligand to prepare a new metal complex by reacting with metal ion Pd(II). The prepared complex was employed as a storage media for carbon dioxide. Different techniques were utilized to examine the physical, chemical, and morphological properties of the prepared composite. Results showed a promising approach for this type of materials in gas storage, which presents a proper solution for gas pollution and global warming issues.

MATERIAL AND METHODS

Sodium fusidate was equipped by SPAIN company as a white, crystalline, and odorless powder of 99.5% purity; it was used without any further purification. The products were characterized by CHNS elemental analysis, ultraviolet-visible (UV-Vis) spectroscopy, Fourier transform infrared (FTIR) spectroscopy, and melting point determination devices. The microanalytical data of the CHNS were collected using AA-680 Shimadzu atomic absorption spectroscopy and Euro EA3000. FTIR spectra of the prepared products were detected via a CsI disc of a Shimadzu and Perkin Elmer spectrometer. Electronic spectra of complexes and their ligands in solution state were recorded on a UV-Vis device of 1800 PC Shimadzu Spectrophotometer.

A 0.177 gm of PdCl₂ solid salt was dissolved in ethanol and added to 10 ml of L-ethanolic solution in a molar ratio of 1:2 with stirring. During the synthesis process, the mixture was heated and refluxed for 3 hr until a precipitate was formed, which was then filtered and multiply washed with DI water to terminate traces of the salt. Finally, the product was dried under a vacuum and crystallized from ethanol, where it was identified using different analytical and physical techniques.

RESULTS AND DISCUSSION

The synthesized complexes formed as colored powder that showed long-time stability when exposed to an open atmosphere. The analytical data and other physical properties of the palladium complex and ligand (L) are summarized in Table 1.

Table 1. Analytical data for the palladium and ligand complex

Comp.	Color	M.P. °C	Yield%	Molar ratio (M:L)	Elemental analysis Found (Calc.)		
					C	H	N
L	White	204-206d	---	---	(69.05)	(8.72)	----
PdL	Brawn	158-160	80	1:2	65.12 (65.46)	7.81 (8.27)	8.64 (9.36)

Table 2. FTIR Absorption data for the ligand and palladium complex

Formal	ν OH	ν C=O (aster)	ν COO ⁻ (asym.) (sym.)	ν C-OH
L	3487, 3417	1712	1550, 1388	1269
PdL	3487, 3417	1716	1529, 1377	1261

The FTIR spectra show beneficial data for the morphology functional groups reflected from the structural compounds. The characteristic frequencies of free ligand and palladium complex were compared and readily designated to the literature [Nakamoto, 2009]. The infrared bands of L showed sharp and medium characteristic absorption bands which occurred at 1550 and 1388 cm^{-1} ; these were assigned to the stretching asymmetric and symmetric ν COO⁻, respectively. The change in the frequency $\Delta\nu$ was equal to 162 cm^{-1} , and three bands at 3487-3417, 1712, and 1269 cm^{-1} resulted in via hydrogen and carboxyl ester groups' vibration. The IR spectra of the complexes $\Delta(\text{COO}^-)$ were very useful in describing the structure of the prepared compound. The ν_{asym} (COO⁻) stretching appeared at 1529 cm^{-1} , while a vibration was observed at 1377 cm^{-1} , which is explained as ν_{sym} (COO⁻). The difference $\Delta\nu$ (COO⁻) proposes bidentate coordination, where $\Delta\nu$ value was less than the ionic compound [Xiao et al., 2019] as shown in Table 2. More evidence of new medium or weak bands appeared at 1261 cm^{-1} in the prepared palladium complex, which is attributed to the ν (C-OH) as shown in Table 2.

The electronic spectrum of the free ligand (L₁) showed three major bands. The first absorption band was at 225 nm and attributed to the inter-ligand transition ($\pi \rightarrow \pi^*$) located on the pi-system. The other absorption band was located at 242 nm and was also gained from the $\pi \rightarrow \pi^*$ transition from another group. The last absorption band is assigned to the $n \rightarrow \pi^*$ electronic location transition on oxygen atoms of carboxylate, ester, and OH groups that appears at 270 nm [Lotfy et al., 2015].

PdL: The electronic spectra of brown complex show bands at 24154 cm^{-1} for PdL that is attributed to $^1A_1g \rightarrow ^1B_1g$ transition (ν_1) and at 26246 cm^{-1} that is attributed to $^1A_1g \rightarrow ^1E_g(\nu_2)$ transitions for square planer geometry [Lotfy et al., 2015]. Another band appeared at 31746 cm^{-1} that could be assigned to charge transfer $L \rightarrow \text{PdCT}$ of L. The measured magnetic moment is zero B.M.; this indicates the formation of a low spin complex. However, conductivity measurements indicate that the complex is nonionic [Lotfy et al., 2015].

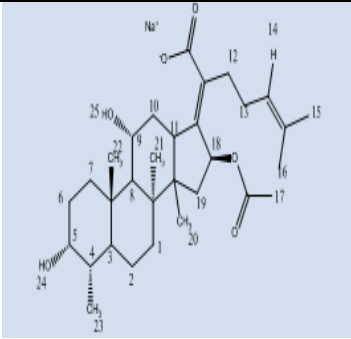
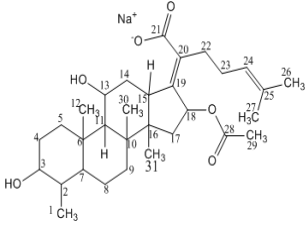
Mode of the ligand and complex are also provided by the $^1\text{HNMR}$ and $^{13}\text{CNMR}$ spectra, which were recorded in DMSO d_6 . The information is reported in Table 4.

The outer surface morphology of the fusidate metal complex was examined via the FESEM technique. Figure 1 shows that the palladium complex has a heterogeneous and porous structure. Furthermore, the FESEM images indicate a mitigated agglomeration of different shapes and sizes of particles. From images, particle size clearly ranged between 44.09-56.29 nm for the

Table 3. Electronic spectra, conductance in DMF solvent, and magnetic moment (B.M.) for the synthesized palladium-ligand complex

Comp.	Absorption cm^{-1}	Assignments	Conductivity μs^{-1}	Suggested geometry
L	37037	$n \rightarrow \pi^*$		
	41322	$\pi \rightarrow \pi^*$	--	----
	44444			
PdL	24154	$^1A_1g \rightarrow ^1B_1g$		
	26246	$^1A_1g \rightarrow ^1Eg$	30	square planner
	31746	$L \rightarrow Pd CT$		

Table 4. ^1H NMR and ^{13}C NMR spectra data of ligand (L)

L: ^1H NMR	^1H NMR
	<p>L: ^1HNMR(DMSO-d_6)δ ppm δ 0.83-0.93 ppm (s,3H,H₂₀-H₂₂ and d,3H,H₂₃) (CH₃ cyclic of L), δ 1.03-1.93ppm to (s,H₁-H₁₀) ppm except peaks in the range δ 3.51-3.59 as (s,H₅ and H₉)ppm to proton on (-CH-OH) groups. Also shows signal as peaks in δ 1.75 and 1.88 ppm to aliphatic methyl proton⁽¹⁾ as a δ 1.75(s,3H,H₁₆) and δ 1.88(s,3H,H₁₅) ppm. Also shows at δ 2.07(s, H₁₂ and H₁₃)ppm to aliphatic methylene (CH₂-CH₂) proton^(2,1), and at δ 5.30-5.35(t,H,H₁₄,H₁₈)ppm. The peaks on δ 2.26 and 2.28(s, 1H, H₁₇)ppm which is ascribed aliphatic methyl on ester group (CH₃-COO-) proton, and peak which appeared on δ 4.28-4.30ppm which corresponding to proton on (-OH) group. The comparison of ^1HNMR spectra of Pd(II) complex formed with the ligand spectrum position of the proton about confirming the coordination, a very little shifting in the proton position of the ligand with these metal complex</p>
L: ^{13}C NMR	^{13}C NMR
	<p>L: ^{13}CNMR(DMSO-d_6)δppm 15.51 (C₁ and C₁₂ CH₃ cyclic of sodium fusidate), 18.74 (C₃₀ and C₃₁ CH₃ cyclic of ligand (L)), 22.14 and 24.94 (C₂₆, C₂₇ and C₂₉ CH₃- aliphatic), 28.74, 29.69 (C₂₂ and C₂₃ CH₂- CH₂ aliphatic), 31.29-35.80 (C₄, C₅, C₉, C₁₄ and C₁₅ CH₂- cyclic of ligand (LI)), 41.94 and 42.14 (C₂ and C₆ CH- cyclic of ligand (LI)), 45.66 (C₁₀, and C₁₇), 48.14 (C₇, and C₁₆ C- cyclic of ligand (LI)), 55.71 (C₁₁), 68.15 (C₁₃, C-OH), 77.75 and 78.94 (C₃ and C₁₈ C-OH), 125.55 and 132.21 (C₂₄ and C₂₅ CH=C(CH₃)₂), 139.51 (C₂₀ C=C), 170.75 and 171.94 (C₂₁ and C₂₈ COO carboxyl).</p> <p>The comparison of ^{13}CNMR spectra of Pd(II) complex formed with the ligand spectrum. There is a shifting in the peak of C=C group to δ 165.61 ppm, and the peak of COO to δ 178.78 ppm group in the ligand with these metal complexes; this is confirming the coordination compound.</p>

prepared complex.

Energy dispersive X-ray spectroscopy (abbreviated as EDS or EDX) was employed to analyze elements and chemically characterize the sample [Mahmood et al., 2021; Ahmed et al., 2018]. It is a type of spectroscopies in which a sample is investigated through interactions between matter and electromagnetic radiation. The X-ray emitted by the matter is analyzed by this technique when reflected from charged particles [Gangadhar et al., 2015]. The spectrum is displayed in Figure 2, and the detected structural peaks are listed in Table 5.

The Brunauer-Emmett-Teller (BET) method was utilized to calculate the specific surface area via nitrogen (N₂) adsorption-desorption isotherms [Vergis et al., 2019]. The adsorbent's porosity gives beneficial information on its physicochemical interactions with adsorbed gas. Thereby, the pore size distributions and nitrogen isotherms of the prepared palladium complex are shown in

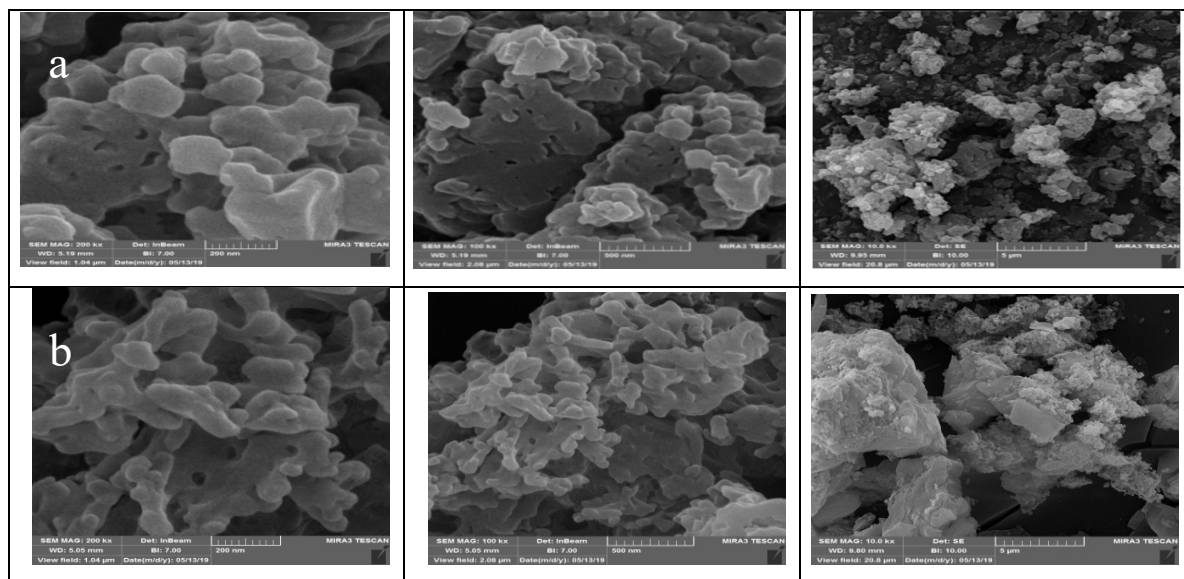


Fig. 1. FE-SEM images of (a) L, (b) PdL complex.

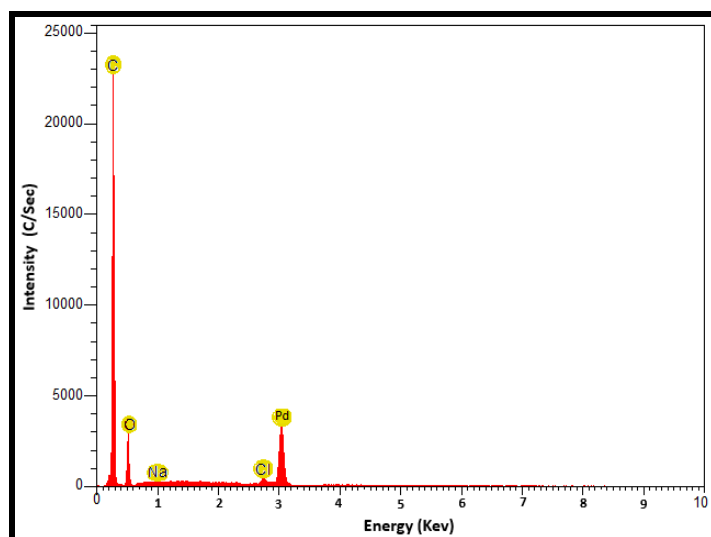


Fig. 2. EDX pattern of Pd complex

Table 5. Energy dispersive X-ray spectroscopy results of Pd complex

Comp.	Carbon	Oxygen	Chloride	Metals
PdL	68.68	19.62	0.43	10.98

Figure 3, where the nitrogen adsorption-desorption curves are overlaid. From the curve, the Pd complex has an adsorption curve of type III and no monolayer formation is identified.

The pore volume and BET surface area were estimated from the nitrogen adsorption-desorption isotherms at $P/P_0 = 0.9$. However, the size and volume of pores were calculated via the Barrett-Joyner-Halenda (BJH) method, and the numerical values were listed in Table 6. It is good to mention that the BET surface area and pore volume were calculated from nitrogen

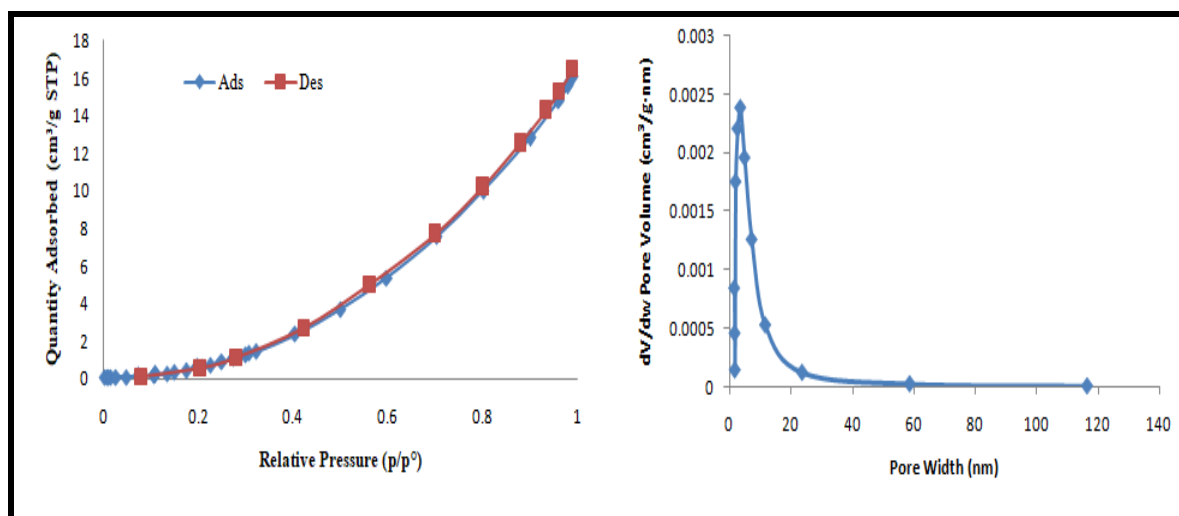


Fig. 3. N₂ adsorption-desorption isotherms and pore size distribution of the Pd-L complex

Table 6. Surface area and pore size distribution of palladium complex obtained by the N₂ adsorption-desorption isotherms

Comp.	SBET (m ² .g ⁻¹)	Pore Volume (cm ³ .g ⁻¹)	Average pore diameter (nm)
PdL	29.321	0.029	2.898

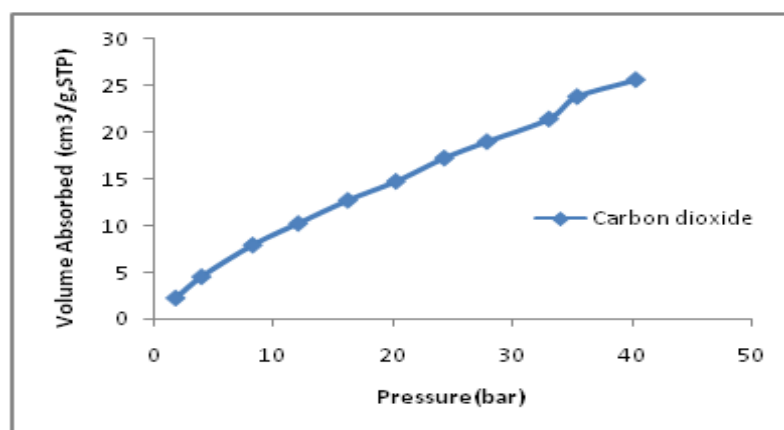


Fig. 4. Adsorption isotherms of CO₂ for PdL complex

adsorption, while the BJH average pore diameter was estimated based on the desorption data.

The gas uptake capability of the synthesized complex was identified via a high-pressure volumetric adsorption apparatus of type H-sorb 2600. The complex was degassed under vacuum and heat using an oven operated at 50 °C for 1h to terminate any trapped solvent or water traces inside the pores. In order to obtain accurate results, the gas uptake examination was replicated using identical conditions for the prepared complex to detect the optimum pressure. Gas adsorption depends on the pore size, metal charge, ligand type, and interaction strength between the adsorbate and adsorbent, such as the hydrogen bonds and Van der Waal forces [Khadilkar and Chavan, 2009; Kalash et al., 2020]. The pore volume plays an important role to find the gas uptake capacity of adsorbent materials, where a large pore volume results in storing higher amounts of gases [Peng et al., 2013]. CO₂ owns a strong quadrupole moment;

Table 7. Gas uptake capacities at 323 K of palladium complex

Comp.	CO ₂ Uptake (cm ³ .g ⁻¹)	CO ₂ Uptake (wt%)
PdL	25.58	5.2

this conducts a remarkable adsorption capacity as it is highly diffusible [Razavian et al., 2014]. The high attraction forces, such as electrostatic (polarization force and surface field-molecular dipole interactions) and Van der Waals forces, may also fulfill high CO₂ uptake [Ahmed et al., 2018; Omer et al., 2020; Satar et al., 2019; Najim et al., 2020; Mousa et al., 2020]. The adsorbed gas volume relationship with pressure for the Pd-L complex is shown in Figure 4 and Table 7.

CONCLUSION

Herein, a palladium complex containing fusidate moiety was synthesized and its chemical structure was established. The palladium complex has particles that vary in shape, size, and diameter. Based on the characterization techniques, the complex had a surface area of 29.321 m²/g, which makes it suitable for many applications. In gas storage, the gas uptake depended on the type of gas, structural metal, surface pore volume, and pore diameter. The synthesized complex was tested for CO₂ uptake and the results show an uptake of 25.58 cm³/g, which equals 5.2 wt.% of the complex. Further investigation is recommended to employ this type of complex for gas storage, which may contribute to finding a solution for the recent CO₂ high levels problem and global warming.

ACKNOWLEDGMENT

The authors like to thank Al-Nahrain University for partially supporting this work.

GRANT SUPPORT DETAILS

The present research did not receive any financial support.

CONFLICT OF INTEREST

The authors declare that there is not any conflict of interests regarding the publication of this manuscript. In addition, the ethical issues, including plagiarism, informed consent, misconduct, data fabrication and/ or falsification, double publication and/or submission, and redundancy has been completely observed by the authors.

LIFE SCIENCE REPORTING

No life science threat was practiced in this research.

REFERENCES

- Al-Furaiji, M.H., Arena, J.T., Maqsood, C., Benes, N., Nijmeijer, A. and McCutcheon, J.R. (2018). Use of forward osmosis in treatment of hyper-saline water. *Desalin. Water. Treat.*, 133; 1-9.
- Al-Furaiji, M., Kadhom, M., Kalash, K., Waisi, B. and Albayati, N. (2020). Preparation of thin-film composite membranes supported with electrospun nanofibers for desalination by forward osmosis. *Drink. Water. Eng. Sci.*, 13(2); 51-7.
- Ahmed, D.S., El-Hiti, G.A., Yousif, E., Ali, A.A. and Hameed, A.S. (2018). Design and synthesis of porous

- polymeric materials and their applications in gas capture and storage: a review. *J. Polym. Res.*, 25(3); 75.
- Alias, M. and Bakir, S. R. (2018) Synthesis, Spectroscopic Characterization and in Vitro Cytotoxicity Assay of Morpholine Mannich Base Derivatives of Benzimidazole with Some Heavy Metals. *Al-Nahrain J. Sci.*, 21(3); 50-60.
- Benson, S. M. and Orr, F. M. (2008). Carbon dioxide capture and storage. *MRS bulletin.*, 33(4); 303-305.
- Curbete, M. and Salgado, H. N. (2015). A critical review of the properties of fusidic acid and analytical methods for its determination. *Crit. Rev. Anal. Chem.*, 46(4); 352-360.
- Fernandes, P. (2016). Fusidic acid: a bacterial elongation factor inhibitor for the oral treatment of acute and chronic staphylococcal infections. *Cold Spring Harb. Perspect. Med.*, 6 (1); a 025437.
- Gangadhar, R., Jaleeli, K. A. and Ahmad, A. (2015). Energy dispersive x-ray analysis of ovine scapular cartilage. *Int. J. Environ. Sci. Technol.*, 4(4); 1195-1198.
- Kalash, K. R., Al-Furaiji, M. H., Waisi, B.I. and Ali, R. A. (2020). Evaluation of adsorption performance of phenol using non-calcined Mobil composition of matter no. 41 particles. *Desalin. Water Treat.*, 198; 232-240.
- Khadilkar, A. and Chavan, S. (2009) Metal Organic Frameworks: Giant Rescuers. *The Bombay Technologist.*, 59; 44-51.
- Lim, K. L., Kazemian, H., Yaakob, Z. and Daud, W. W. (2010). Solid-state materials and methods for hydrogen storage: a critical review. *Chem. Eng. Technol.*, 33(2); 213-226.
- Lotfy, H. M., Salem, H., Abdelkawy, M. and Samir, A. (2015). Spectrophotometric methods for simultaneous determination of betamethasone valerate and fusidic acid in their binary mixture. *Spectrochim. Acta A Mol. Biomol. Spectrosc.*, 140; 294-304.
- Mahmood, Z. N., Alias, M., El-Hiti, G. A. R., Ahmed, D. S. and Yousif, E. (2021). Synthesis and use of new porous metal complexes containing a fusidate moiety as gas storage media. *Korean J. Chem. Eng.*, 38(1); 179-186.
- Morris, R. E. and Wheatley, P. S. (2008) Gas storage in nanoporous materials. *Angew. Chem. Int. Ed.*, 47(27); 4966-4981.
- Mousa, O. G., Yousif, E., Ahmed, A. A., El-Hiti, G. A., Alotaibi, M. H. and Ahmed, D. S. (2020). Synthesis and use of carvedilol metal complexes as carbon dioxide storage media. *Appl. Petrochem. Res.*, 10; 157-164. <https://doi.org/10.1007/s13203-020-00255-7>.
- Najim, L. H., El-Hiti, G. A., Ahmed, D. S., Mohammed, A., Alotaibi, M. H. and Yousif, E. (2020). Valsartan metal complexes as capture and reversible storage media for methane. *Appl. Petrochem. Res.*, 10; 77-82. <https://doi.org/10.1007/s13203-020-00247-7>
- Nakamoto, N. (2009). *Infrared and Raman Spectra of Inorganic and Coordination Compounds*. New York, John Wiley & Sons Inc., 6th Ed.
- Omer, R. M., Al-Tikrity, E. T. B., El-Hiti, G. A., Alotibi, M. F., Ahmed, D. S. and Yousif, E. (2020) Porous Aromatic Melamine Schiff Bases as Highly Efficient Media for Carbon Dioxide Storage. *Processes*, 8; 17. <https://doi.org/10.3390/pr8010017>
- Owusu, P. A. and Asumadu-Sarkodie, S. A. (2016) review of renewable energy sources, sustainability issues and climate change mitigation. *Cogent Eng.*, 3(1); 1167990[†]
- Peng, Y., Krungleviciute, V., Eryazici, I., Hupp, J. T., Farha, O. K. and Yildirim, T. (2013) Methane storage in metal-organic frameworks: current records, surprise findings, and challenges. *J. American Chem. Soc.*, 135(32); 11887-11894[†]
- Razavian, M., Fatemi, S. and Masoudi-Nejad, M. A. (2014). Comparative study of CO₂ and CH₄ adsorption on silicalite-1 fabricated by sonication and conventional method. *Adsorpt. Sci. Technol.*, 32(1); 73-87.
- Safarov, N. and Atkinson, C. (2017). Natural gas storage valuation and optimization under time-inhomogeneous exponential Lévy processes. *Int. J. Comput. Math.*, 94(11); 2147-2165[†]
- Satar, H. A., Ahmed, A. A., Yousif, E., Ahmed, D. S., Alotibi, M. F. and El-Hiti, G.A. (2019). Synthesis of Novel Heteroatom-Doped Porous-Organic Polymers as Environmentally Efficient Media for Carbon Dioxide Storage. *Appl. Sci.*, 9; 4314. <https://doi.org/10.3390/app9204314>
- Vergis, B. R., Kottam, N., Krishna, R. H. and Nagabhushana B. M. (2019). Removal of Evans Blue dye from aqueous solution using magnetic spinel ZnFe₂O₄ nanomaterial: Adsorption isotherms and kinetics. *Nano struct. Nano objects.* 18; 100290.
- Waisi, B. I., Karim, U. F., Augustijn, D. C., Al-Furaiji, M. H. and Hulscher, S. J. (2015). A study on the quantities and potential use of produced water in southern Iraq. *Water science and technology:*

- Water Suppl., 15(2); 370-376.
- Whitby, M. (1999). Fusidic acid in the treatment of methicillin-resistant *Staphylococcus aureus*. *Int. J. Antimicrob. Agents*, 12; S67-S71.
- Xenias, D. and Whitmarsh, L. (2018). Carbon capture and storage (CCS) experts' attitudes to and experience with public engagement. *Int. J. Greenh. Gas Control.*, 78; 103-116.
- Xiao, Q. Q., Liu, D., Wei, Y. L. and Cui, G. H. (2019). Two new ternary Mn (II) coordination polymers by regulation of aromatic carboxylate ligands: Synthesis, structures, photocatalytic and selective ion-sensing properties. *J. Solid State Chem.*, 273; 67-74.